PAPER

Check for updates

D−π−A type conjugated indandione derivatives: ultrafast broadband nonlinear absorption responses and transient dynamics†

Lu Chen,[a] Xingzhi Wu, [iD] *[b] Zhongguo Li,[c] Ruipeng Niu,[d] Wenfa Zhou, [iD] [d] Kun Liu,[a] Yingfei Sun,[a] Zhangyang Shao,[a] Junyi Yang [iD] *[a] and Yinglin Song [iD] *[ad]

The ultrafast nonlinear optical response of two 1,3-indandione derivatives (INB3 and INT3) was systematically investigated by the femtosecond Z-scan and pump-probe technique at multiple visible and near infrared wavelengths. Both compounds show strong broadband nonlinear absorption (NLA) and different wavelength-dependent two-photon absorption (TPA) characteristics in the range of 650–1100 nm. The TPA cross section of trithiophene-based compound INT3 was found to be larger than that of triphenylamine-based compound INB3 in the red region (650–800 nm), which is attributed to its longer π-conjugated structure and better molecular planarity. Interestingly, the effective NLA of INB3 was found to be larger than INT3 in the NIR region (800–1100 nm), which is related to the excited state absorption (ESA) induced by TPA. The ultrafast dynamics of both compounds were investigated by femtosecond transient absorption spectroscopy, which revealed a broadband ESA including several relaxation processes. This work extends nonlinear optical research on indandione derivatives, and the results suggest that these derivatives are promising candidates for optical limiting applications.

1. Introduction

Near-infrared (NIR) nonlinear materials are increasingly popular in photoelectric sensing and other fields due to their minimal photodamage to samples and minimal tissue penetration depth.[1] Organic nonlinear materials have great advantages, such as low cost, wide spectral response and easy modification/tailoring of molecular structure. They have promising applications in all optical switching,[2–4] optical limiting devices,[5,6] bioimaging, optical communication and information storage.[7–9] In addition, organic molecular materials containing π-conjugated structures play a decisive role in enhancing the optical nonlinear properties.[10–12] As a promising type of π-conjugated molecule, indandione derivatives have attracted much attention due to their easy synthesis and significant second- and third-order optical nonlinearity.[13–15] Interestingly, these types of compounds exhibit strong nonlinear optical (NLO) responses due to the introduction of

[a]School of Physical Science and Technology, Soochow University, Suzhou 215006, People's Republic of China

[b]School of Physical Science and Technology, Suzhou University of Science and Technology, Suzhou 215009, People's Republic of China

[c]School of Electronic and Information Engineering, Changshu Institute of Technology, Changshu 215500, China

[d]Department of Physics, Harbin Institute of Technology, Harbin 150001, People's Republic of China

† Electronic supplementary information (ESI) available. See DOI: 10.1039/d2ra00349j

bilateral donor and acceptor groups, strong intermolecular interactions and TPA resonance in π-conjugated systems.[16–18]

The introduction of electron donors and acceptors into the molecular structure increases the difference in the dipole moment between the excited and ground states, which enhances the polarization of the whole molecule under an external electric field through intramolecular charge transfer (ICT), hence greatly improving the second- or third-order nonlinear effects of materials.[19,20]

Under laser irradiation at longer wavelengths, ground state electrons could be promoted to the excited state by simultaneously absorbing two incident photons. After that, ESA shows its effect until the molecular system relaxes to the ground state. The cooperating effect of TPA and ESA could enhance the overall nonlinear optical absorption in the whole spectral region.[21] Thus, it is feasible to achieve a broader spectral response range by proper design of molecular structures, including adjusting the molecular length, ICT and molecular symmetry by introducing different donors and acceptors. At present, indandione research is still confined to theoretical simulations[22] and some low-order nonlinear responses, and in-depth analysis of its high-order NLO is still very rare.[15,23–27]

Based on these facts, two compounds, INB3 (2-[4-di(*p*-toly-lamino)benzylidene]-1*H*-indene-1,3(2*H*)-dione) and INT3 (2-[(2,2′:5′2″-terthiophene-5-yl)methylene]-1*H*-indene-1,3(2*H*)-dione), were synthesized by introducing triphenylamine and terthiophene as donor groups. In this paper, the higher-order NLO response of 1,3-indandione dissolved in DMSO (dimethyl

sulfoxide) was investigated experimentally by femtosecond Z-scan experiments and transient absorption (TA) spectroscopy. The results indicated that the introduction of triphenylamine and terthiophene exhibits a great effect on the ESA spectrum and ultrafast dynamics. Both compounds exhibit excellent NLO responses in a wide spectral region from visible to NIR (650–1100 nm). This indicates that INB3 and INT3 are potential materials for applications such as near infrared optical sensing and modulation in the photoelectric area (Scheme 1).

2. Experimental

2.1 Synthesis and spectroscopic characterization of INB3 and INT3

2.1.1 Synthesis of 2-[4-di(*p*-tolylamino)benzylidene]-1*H*-indene-1,3(2*H*)-dione (INB3). A mixture of 4-di-*p*-tolylamino-benzaldehyde (1 g, 3.32 mmol) and 1,3-indonedione (0.485 g, 3.32 mmol) was dissolved in 100 mL of ethanol. The solution was added in sequence to a 200 mL two-sipped flask and stirred magnetically until the solution was reddish-brown when completely dissolved. Then, several drops of triethylamine were added, and the solution turned dark wine red. The reaction was stirred at room temperature, and the reaction process was tracked by thin layer chromatography (TLC). The reaction time was approximately 5 h (after the end of the reaction, the color of the solution was still dark wine red, and there was no precipitation throughout the reaction process). Dry material was prepared with an appropriate amount of silica gel. Compound INB3 (895 mg, 62.8%) was obtained by column chromatography separation. ^{1}H NMR δ/ppm (600 MHz, DMSO): 8.472–8.458 (d, 2H, J = 8.4 Hz), 7.913–7.880 (m, 4H), 7.678 (s, 1H), 7.265–7.252 (d, 4H, J = 7.8 Hz),7.162–7.149 (d, 4H, J = 7.8 Hz), 6.785–6.771 (d, 2H, J = 8.4 Hz),2.238 (s, 6H). ^{13}C NMR δ/ppm (150 MHz, DMSO): 190.61,189.44,153.22, 146.03, 142.85, 142.08, 142.00, 139.70, 137.40, 136.01, 135.87, 135.68, 131.05, 127.17, 124.73, 124.61, 123.08, 122.99, 117.01, 21.05. LC-MS (ESI) *m/z*: found: 430.15; calcd for $C_{30}H_{23}O_2N$ ([M]$^+$): 429.52.

2.1.2 Synthesis of 2-[(2,2′:5′2″-terthiophene-5-yl)methy-lene]-1*H*-indene-1,3(2*H*)-dione (INT3). A mixture of 2,2′:5′2″-terthiophene-5-carbaldehyde (1.01 g, 5 mmol) and 1,3-indone-dione (0.73 g, 5 mmol) was placed in a 100 mL round-bottom flask. Then, 30 mL of anhydrous ethanol was added and

stirred magnetically to completely dissolve it. Four drops of triethylamine were added, and reflux was heated for 4 h. The reaction was stirred at room temperature, and the reaction process was tracked by thin layer chromatography (TLC). When TLC showed that no product was formed, potassium *tert*-but-oxide (0.55 g, 5 mmol) was added, and reflux was continued. The solution changes from yellow to brick red, and TLC shows that the reaction is successful. The reaction time was approximately 4 h (after cooling to room temperature, the brick red suspension was obtained, which was filtered and washed twice with a small amount of anhydrous ethanol to obtain the reddish-brown coarse product). Compound INT3 (890 mg, 44.1%) was obtained by column chromatography separation. ^{1}H NMR δ/ppm (600 MHz, DMSO): 8.220–8.213 (d, 1H, J = 4.2 Hz), 8.068 (s, 1H), 7.949–7.919 (m, 4H), 6.673–6.667 (d, 1H, J = 3.6 Hz),6.656–6.649 (d, 1H, J = 4.2 Hz), 6.632–6.623 (d, 1H, J = 5.4 Hz),7.486–7.481 (d, 1H, J = 3.0 Hz), 7.433–7.427 (d, 1H, J = 3.6 Hz), 7.168–7.154 (t, 1H,J = 4.2 Hz). ^{13}C NMR δ/ppm (150 MHz, DMSO): 189.85, 189.67, 148.91, 146.14, 141.81, 140.38, 139.19, 136.09, 136.01, 135.97, 135.88, 135.83, 134.44, 129.18, 128.79, 127.25, 126.12, 26.00, 125.78, 113.72, 123.23, 123.08. LC-MS (ESI) *m/z*: (ESI) found: 404.87; calcd for $C_{19}H_{16}O_5$ ([M]$^+$): 404.53 (Scheme 2).

2.2 Quantum chemical calculations

The Gaussian 09 program package was used for density functional theory (DFT) to investigate the influence of molecular structure on the NLO properties of these two compounds. The B3LYP/6-31G model was applied to optimize the structures of all the molecular systems. The energy and electron cloud distribution of frontier molecular orbitals were calculated (Fig. 2). To further analyze the electron transition, density functional theory (DFT)[28] was performed using the CAM-B3LYP functional[29] and the B3LYP/6-311G(d) basis set. The electrons transfer from the donor (three thiophene or triphenylamine groups) to the acceptor (1,3-indandione group) in both compounds. The type of electron transition can be characterized by hole electron analysis using the Multiwfn 3.7 program.[30]

2.3 Transient absorption measurement

The laser source of femtosecond TA spectroscopy was the same as that used in the Z-scan measurement. In femtosecond TA measurements, the pump wavelength was set to 480 nm. The probe wavelength window covers a range from 480 nm to
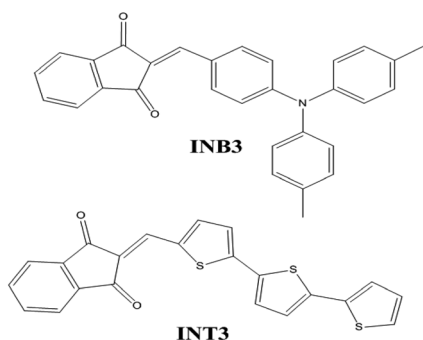
Scheme 1 Molecular structure of INB3 and INT3.
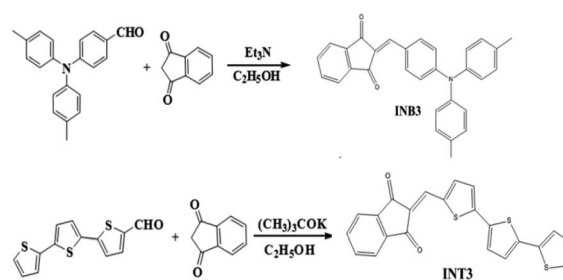
Scheme 2 Synthetic route of molecules INB3 and INT3.

1100 nm. The time resolution of the TA system was approximately 250 fs. The pump fluence was kept below 8 mW to suppress high-order relaxation processes. Details of TA measurement can be found in a previous report.[31] Both compounds were dissolved in DMSO at the same concentration (1.18×10^{-4} mol L^{-1}) at room temperature. The sample solution was contained in 2 mm quartz cell.

2.4 Nonlinear absorption experiments

The ultrafast nonlinear absorption of INB3 and INT3 compounds was characterized by the open-aperture Z-scan technique under the excitation of femtosecond laser pulses. Optical parametric amplifier (OPA) (light conversion ORPHEUS) pumped by a Yb:KGW femtosecond fiber laser (light conversion) was employed as the laser source, and the wavelength of the output beam could be adjusted from 650 nm to 1100 nm. The pulse duration and repetition rate of the laser beam are 190 fs and 20 Hz, respectively. Both compounds were dissolved in dimethyl sulfoxide (DMSO) at a concentration of 3.3×10^{-3} mol L^{-1}, and the sample solution was placed in 2 mm thick quartz sample cells. In the Z-scan experiment, the NLO effect of the solvent was measured as the background, and nonlinear absorption of the compounds was obtained by subtracting the solvent background signal from the solution signal in data processing.

3. Results and discussion

3.1 UV-vis absorption and fluorescence spectra

The UV-vis absorption spectra and fluorescence spectra of the two 1,3-indandione derivatives are shown in Fig. 1. The measurements were made in DMSO solution at a concentration of 5.9×10^{-5} mol L^{-1} at room temperature. The results show that the absorption peaks of INB3 and INT3 are located at 492 nm and 504 nm, respectively. The absorption peak of INT3 has a certain redshift compared to INB3, indicating a small energy gap in INT3, which is also confirmed by DFT calculations. When both were excited at the absorption peak wavelengths, the fluorescence signal of INB3 was much weaker than that of INT3. In addition, the emission spectral range of INB3 is much broader, suggesting distinct dual emission from the locally excited state (LES) and ICT state.
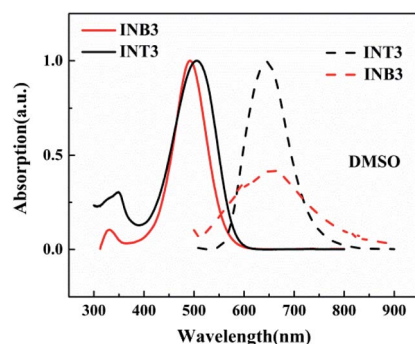
3.2 Quantum chemical calculation

The optimal structure and the distribution of frontier molecular orbitals of INB3 and INT3 are displayed in Fig. 2. From the optimization structure, one can find that the three benzene rings of INB3 are not in the same plane, while the 1,3-indandione group of INT3 forms a planar conjugated system with the thiophene unit.[32,33] As we introduced before, in both compounds, the indandione group acts as an acceptor due to its strong electron-withdrawing ability, while terthiophene and triphenylamine act as donors. In the INB3 and INT3 molecular systems, electrons are transferred from trithiophene and triphenylamine groups to 1,3-indendione, respectively, and there is a significant ICT in both molecules. The degree of planarity affects the length of the π-electron system and the polarizability of electrons,[34] and the effect of the torsional angle between rings may be able to promote the contribution of ICT. Quantitative calculations also show that INT3 shows better planarity and a smaller band gap, while INB3's ICT is more pronounced, and these two mechanisms are expected to have different modulation effects on its nonlinear absorption.

3.3 Transient absorption spectrum

The results of femtosecond transient absorption spectra (TAS) of the two compounds are displayed in Fig. 3, in which the positive signal represents ESA at a specific wavelength. For INB3, with excitation from the pump pulse, the ESA signal emerges at approximately 900 nm, and a strong negative signal covers a wide spectrum from 500 to 800 nm (0.3 ps). The strong negative signal may originate from ground state bleaching and stimulated emission (SE) at corresponding wavelengths (Fig. 1). After that, one can observe a redshifting of the decreasing SE band with a distinct change in the TAS. At 3.0 ps, the ESA signal at approximately 900 nm becomes negative, and a new ESA rises at approximately 570 nm, which turns the previous negative signal positive. The ultrafast sign change of the TAS signal in INB3 could be considered the sum effect of ESA and SE. The strong SE in the INB3 sample undergoes a significant redshift, with its peak moving from 580 nm at 0.3 ps to 840 nm at 9.0 ps. It should be noted that this redshifting of SE in the first singlet state also agrees with the broadband fluorescence emission in INB3 (Fig. 1). Meanwhile, the TAS of INT3 displays a stable ESA
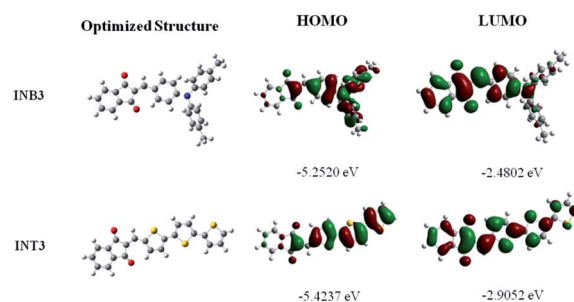

Fig. 1 UV-vis absorption spectra (solid lines) and fluorescence emission spectra (dashed lines) of INB3 (red) and INT3 (black).

Fig. 2 Frontier molecular orbital distributions of INB3 and INT3. Electrons transfer from the highest occupied molecular orbital (HOMO) to the lowest unoccupied molecular orbital (LUMO).
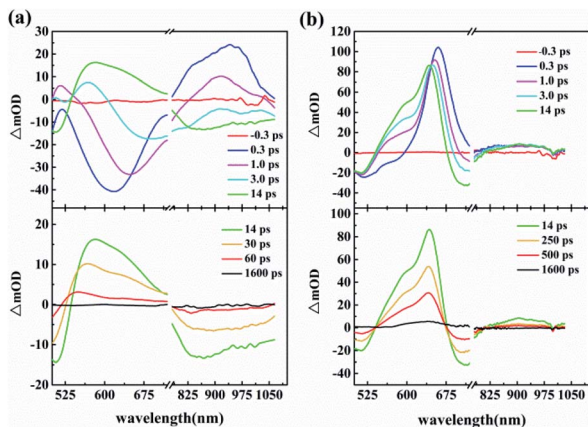
Paper

Fig. 3 Transient absorption spectra of INB3 (a) and INT3 (b) in DMSO at 480 nm under 190 fs excitation.

band with a slight blueshift of its peak from 670 (0.3 ps) to 640 nm (14.0 ps) and a sub-ESA peak rising at approximately 575 nm (from 1.4 ps). Similar to the TAS of INB3, the sum effect of strong SE (peaks at 650 nm according Fig. 1) and ESA results in a negative signal at 720 nm.

To further analyze the ultrafast dynamics of the two compounds, global and target analysis is employed to extract several relaxing processes from the TAS based on the above discussions,[11,35–38] and the results are listed in Table 1. For INB3, ultrafast absorption is established within a pulse duration after excitation, which is beyond the instrument response time (0.25 ps). This ultrafast signal is assigned to the formation of a locally excited state (LES). Afterwards, an ICT excited state is populated with an internal conversion time τ_2 from the LES. The TAS in this ICT state is characterized by a strong ESA band in the visible region and SE in the NIR region, which plays a key role in the sign switching of the TAS signal in INB3. The following process with lifetimes τ_3 is assigned to cooling in the ICT state characterized by a continuous redshifting of the SE signal. Finally, the electrons relaxed back to the ground state from the ICT state with lifetime τ_4. The situation in INT3 is less complicated than that in INB3, and we extract four decay processes with four lifetimes (τ_1–τ_4) listed in Table 1. Four equivalent energy levels and their corresponding evolution associated difference spectra (EADS) are sequentially arranged in order to compare several dynamic processes more accurately (Fig. S7†). Similar to INB3, the ultrafast decay beyond the time resolution of our experiment (τ_1) is assigned to an ultrafast relaxation process in LES after excitation. Meanwhile, τ_2 is assigned to the internal conversion from the LES to the ICT state, which is followed by the relaxation time in the ICT state

and finally relaxation back to the ground state with lifetime τ_4. Based on the above discussion, the kinetic traces of INB3 (500 nm, 580 nm and 630 nm) and INT3 (532 nm, 580 nm and 670 nm) were extracted from TAS and are displayed in Fig. 4, in which solid lines represent the fitting results. Furthermore, simplified energy models for both compounds are provided in Fig. 5.

3.4 Femtosecond open aperture Z-scan experiment

To explore the third-order NLO properties of the two compounds, femtosecond open-aperture (OA) Z-scan measurements were carried out at different laser intensities at wavelengths ranging from 650–1100 nm. The signal of pure solvent was measured to ensure that the solvent absorbing background could be neglected in the experiment. Both compounds show high linear transmittance (INB3 $\geq$ 97%, INT3 $\geq$ 98%) at experimental wavelengths. The results at 650 nm and 1030 nm are shown in Fig. 6, while the results for other wavelengths can be found in the ESI.†

It is known that the OA Z-scan measures the intensity-dependent transmittance of the incident laser, which reflects the third-order nonlinear absorption of the samples. Considering the low repetition rate and high transmittance of samples, the thermal effect of the samples can be ignored in the experiment. As shown in Fig. 6, the OA Z-scan curves show a single valley at the zero point (focus of the lens). The results indicate that the transmittance of both samples decreases as the incident laser intensity increases, which is a typical characteristic of TPA or ESA. In addition, six wavelengths (700 nm, 750 nm, 800 nm, 900 nm, 950 nm, 1100 nm) were selected as examples to show the difference of strength of nonlinear absorption between INB3 and INT3 at the same excitation energy (Fig. 7). It is obvious that the OA curves in the range of 650–800 nm of INT3 have deeper valleys than those of INB3, suggesting significantly stronger nonlinear absorption in INT3. However, the situation is totally opposite when the laser wavelength is tuned to 800–1100 nm, where INT3 displays larger nonlinear absorption. Obviously, the different molecular structures modify the wavelength response of nonlinear absorption in INB3 and INT3 compounds. To further study the ultrafast nonlinear absorption in INB3 and INT3, numerical simulation is employed.
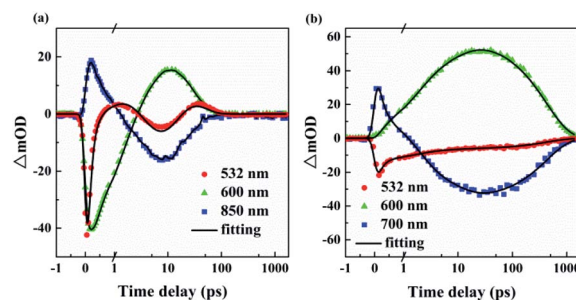
Table 1 Fitting results of dynamic traces for INB3 and INT3 after photoexcitation. The error range of theoretical fitting is about 15%

Sample	τ_1 (ps)	τ_2 (ps)	τ_3 (ps)	τ_4 (ps)
INB3	<0.25	0.9	4.3	24.7
INT3	<0.25	1.6	8.8	424.1

Fig. 4 The kinetic traces of INB3 (a) and INT3 (b) at different wavelengths.
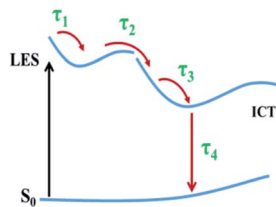
Fig. 5 The energy relaxation diagram for INB3 and INT3.

Note that both INB3 and INT3 samples display extremely high linear transmittance in our Z-scan experiment. Hence, the nonlinear absorption we observed cannot originate from reverse saturable absorption (RSA). The main mechanism of nonlinear absorption in the Z-scan measurement is assigned to TPA and two-photon absorption-induced excited-state absorption (TPA-ESA). The total absorption of the sample (α) can be written as $\alpha = \alpha_0 + \beta_{eff}I$, where α_0 represents the linear absorption coefficient and β_{eff} is the effective third-order nonlinear absorptive coefficient. To gain deep insight into the ultrafast nonlinear absorption in these compounds, OA Z-scan curves at various intensities were measured and the effective third-order nonlinear absorptive coefficients β_{eff} were extracted (Fig. 6(c) and (f)). At 650 nm, β_{eff} of INB3 basically remains unchanged at different laser intensities, while β_{eff} of INT3 increases linearly with the incident laser intensity (Fig. 6(c)). The results indicate that the main nonlinear absorption in INB3 is TPA since pure TPA is independent of laser intensity. However, considering the linearly increasing β_{eff} in INT3, a higher-order (fifth-order) nonlinear absorption may play a key role in INT3.[39,40] Furthermore, the excitation wavelength here (650 nm) is too short for three-photon absorption; hence, the fifth-order nonlinear absorption in INT3 is attributed to TPA-ESA.[34,41] On the other hand, when the incident wavelength is tuned to 1030 nm, β_{eff} of both samples displays a slight increase with increasing laser intensity, indicating a dominant

contribution from pure TPA in the entire nonlinear absorption. Based on the above discussions, the fifth-order optical nonlinearity in these compounds is considered, and we express the effective third-order nonlinear absorptive coefficient β_{eff} as $\beta_{TPA} + \gamma I$. Hence, the absorption coefficient of material (α) can be further expressed as $\alpha = \alpha_0 + \beta_{TPA}I + \gamma I^2$, where α_0 represents the linear absorption coefficient, β_{TPA} is the TPA coefficient, and γ represents the fifth-order nonlinear absorption coefficient. According to equation $\sigma_{TPA} = \hbar\omega\beta_{TPA}/N$, the TPA cross sections can be obtained from the Z-scan results. Here, $\hbar$ is reduced Planck's constant, ω is angular frequency and N is the number of particles per unit volume. Both β_{TPA} and γ can be obtained by theoretically fitting the Z-scan curves based on Sheik Bahae's theory,[42] and the fitting results of the two compounds are summarized in Table 2.

One can find that the two 1,3-indandione derivatives show distinct NLO behavior. When the incident wavelength is shorter than 800 nm, INT3 displays stronger nonlinear absorption than INB3. The largest TPA and TPA-ESA of INT3 are observed at 650 nm ($\sigma_{TPA} = 262$ GM, $\gamma = 15 \times 10^{-28}$ m^3 W^{-2}), which agrees with the results in UV linear absorption and TAS. The strong TPA and TPA-ESA are attributed to the good molecular planarity and small band gap of INT3, which greatly improves the NLO response of the molecule toward laser excitation. With increasing incident wavelength, TPA and TPA-ESA in INT3 gradually decrease. When the excitation wavelength is longer than 900 nm, there is a significant rise in TPA in INB3, which peaks at 1030 nm with $\sigma_{TPA} = 166$ GM. The enhanced TPA in INB3 at 1030 nm may originate from the resonance of the TPA transition between HOMO–LUMO.[43] In addition, INB3 exhibits an excellent NLO response in the NIR region due to its broadband ultrafast ESA, which is also consistent with the TAS results. Both compounds show strong nonlinear absorption in a wide spectral region from visible to NIR, in which the NLO absorption at different wavelengths could be tuned via proper adjustment of the molecular structures. The strong NLO
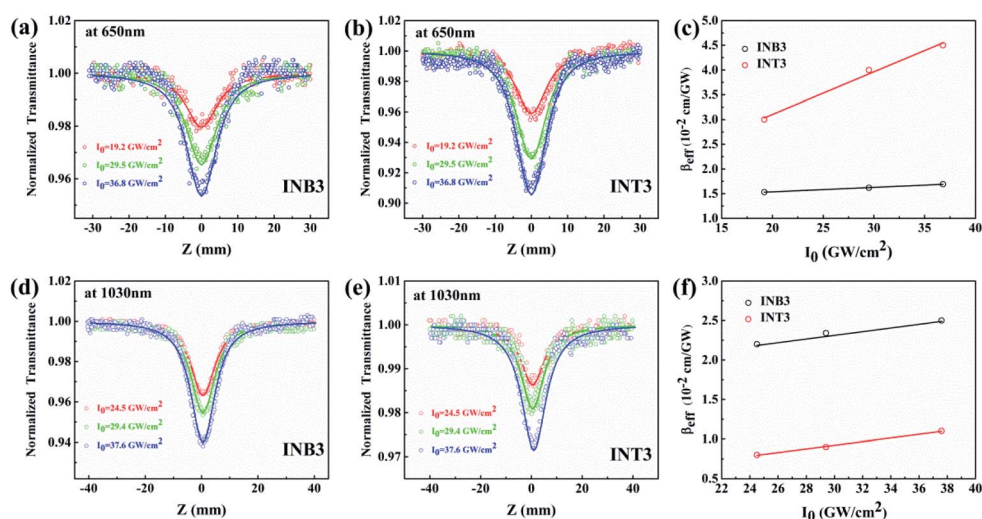

Fig. 6 OA Z-scan experiment of INB3 and INT3 at 650 nm (a–e) and 1030 nm (d–f), respectively. Example of the intensity dependence of the nonlinear absorption coefficient for two compounds. The dots are experimental points and the solid lines are theoretical fitting curves.
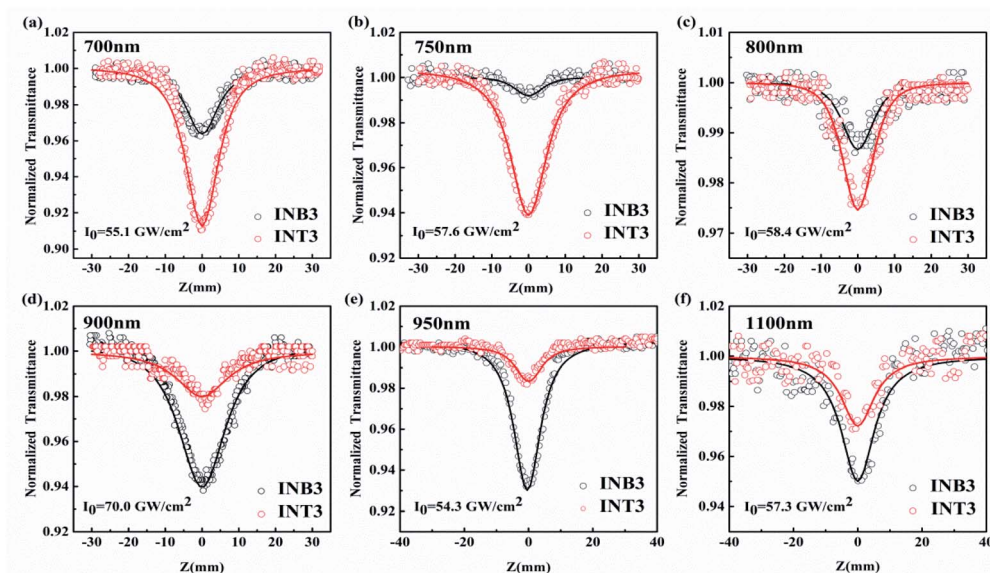
Fig. 7 OA Z-scan experiment at 700 nm, 750 nm, 800 nm, 900 nm, 950 nm, and 1100 nm, respectively. The dots are experimental points and the solid lines are theoretical fitting curves.

Table 2 TPA cross sections and γ at 650–1100 nm fitted from Z-scan experimental data. The error range of theoretical fitting is about 10%

Wavelength (nm)	Sample	β_{TPA} ($\times 10^{-14}$ m W^{-1})	σ_{TPA} (GM)	γ ($\times 10^{-28}$ m^3 W^{-2})
650	INB3	10	154	—
	INT3	17	262	15
700	INB3	4.5	65	—
	INT3	10	143	6.0
750	INB3	0.5	7.0	—
	INT3	8.0	107	3.3
800	INB3	0.2	10	1.4
	INT3	3.5	38	1.3
900	INB3	6.0	67	2.0
	INT3	1.5	17	1.0
950	INB3	13	137	3.0
	INT3	2.0	21	0.5
1030	INB3	17	166	4.0
	INT3	8.5	83	0.5
1100	INB3	9.0	82	3.0
	INT3	5.0	46	0.3

ordinate is expressed as a normalized transmittance, with a linear transmittance of 1 when the sample has not received pump excitation. The decrease at zero time means that the transmittance of the sample is obviously decreased after being excited, which corresponds to the positive nonlinear absorption. In Fig. S16(a),† INB3 drops suddenly after zero delay, and the steep valley is consistent with our 190 fs pulse.[48] TPA is a transient electron response process, and the results show that TPA dominates the nonlinear absorption of INB3. However, in Fig. S16(b),† INT3 returns to the ground state process after a period, and its attenuation life is significantly longer than the pulse width. In addition to TPA, INT3 also has a higher order ESA. Therefore, we determined that the nonlinear response of INT3 comes from a TPA-ESA. A pump–probe experiment verifies the reliability of the Z-scan results and corresponds to the dynamic process of TA. From the absorption kinetics curves of the two molecules, it can be seen that after zero delay, INB3 first appears as a saturation signal soon, then begins to appear as a reverse saturation signal after approximately 1 ps, and finally goes through a long recovery process. INT3 is a process in which a decreasing reverse saturation signal first appears, then slowly recovers and finally returns to the ground state.

responses of INB3 and INT3 suggest that they are suitable for applications such as laser modulators in specific wavelength regions.

To further verify the mechanism of nonlinear absorption, a degenerate pump-probe experiment was carried out. Details of the relevant experiment can be reported in.[44] Pump–probe experiments can provide dynamic processes of nonlinear absorption and can be considered an advanced alternative to the optical Kerr effect technique.[45] Pump–probe experiments have proven to be one of the powerful tools for studying optical nonlinearity.[46,47] The nonlinear absorption kinetic traces of the two compounds were recorded, as shown in Fig. S16.† The solvent showed no obvious nonlinear absorption signal. The

4. Conclusions

In summary, the NLO response at different wavelengths of two 1,3-indandione derivatives was studied. Both compounds exhibit broadband and strong nonlinear absorption from the visible to NIR region. The NLO properties of both molecules originate from the transfer of delocalized π-electrons from the donor group (terthiophene or triphenylamine) to the acceptor group (1,3-indandione). The NLO response of INT3 at 650–800 nm is better than that of INB3 because it has better molecular planarity and longer π-conjugate length.

Approaching to the NIR region (800–1100 nm), both molecules also show better NLO response due to two-photon resonance, while INB3 exhibited slightly better NLO response than INT3 in the NIR region due to its broadband ESA. Overall, the nonlinear absorption of indandione derivatives at different wavelengths can be modified by introducing the proper substituted groups. This result indicated that INB3 and INT3 may be promising materials for RSA applications in the visible and NIR region, such as optical limiters.

Conflicts of interest

There are no conflicts to declare.

Acknowledgements

References

1 X. Zhang, Y. Xiao, J. Qi, J. Qu, B. Kim, X. Yue and K. D. Belfield, Long-wavelength, photostable, two-photon excitable BODIPY fluorophores readily modifiable for molecular probes, *J. Org. Chem.*, 2013, **78**(18), 9153–9160.

2 Y. Sun, Y. Liu, G. zhao, X. Zhou, Q. Zhang and Y. Deng, Controlled formation of Ag/poly(methyl-methacrylate) thin films by RAFT technique for optical switcher, *Mater. Chem. Phys.*, 2008, **111**(2), 301–304.

3 W. Liu, C. Yang, M. Liu, W. Yu, Y. Zhang, M. Lei and Z. Wei, Bidirectional all-optical switches based on highly nonlinear optical fibers, *Europhys. Lett.*, 2017, **118**(3), 34004.

4 P. Karami and H. K. Salehani, Designing Sagnac all-optical interference switch based on nonlinear photonic crystal, *Optik*, 2021, **241**, 167004.

5 D. Dini, M. J. F. Calvete and M. Hanack, Nonlinear Optical Materials for the Smart Filtering of Optical Radiation, *Chem. Rev.*, 2016, **116**(22), 13043–13233.

6 A. Nevejina-Sturhan, O. Werhahn and U. Siegner, Low-threshold high-dynamic-range optical limiter for ultra-short laser pulses, *Appl. Phys. B*, 2002, **74**, 553–557.

7 K. B. Manjunatha, R. Rajarao, G. Umesh, B. Ramachandra Bhat and P. Poornesh, Optical nonlinearity, limiting and switching characteristics of novel ruthenium metal–organic complex, *Opt. Mater.*, 2017, **72**, 513–517.

8 A. J. Almosawe and H. L. Saadon, Nonlinear optical and optical limiting properties of new structures of organic nonlinear optical materials for photonic applications, *Chin. Opt. Lett.*, 2013, **11**(4), 041902.

9 P. S. Patil, S. R. Maidur, S. V. Rao and S. M. Dharmaprakash, Crystalline perfection, third-order nonlinear optical properties and optical limiting studies of 3, 4-Dimethoxy-4′-methoxychalcone single crystal, *Opt. Laser Technol.*, 2016, **81**, 70–76.

10 M. O. Senge, M. Fazekas, E. G. A. Notaras, W. J. Blau, M. Zawadzka, O. B. Locos and E. M. Ni Mhuircheartaigh, Nonlinear Optical Properties of Porphyrins, *Adv. Mater.*, 2007, **19**(19), 2737–2774.

11 J. Jia, X. Zhang, Y. Wang, Y. Shi, J. Sun, J. Yang and Y. Song, Enhanced Two-Photon Absorption of Cross-Conjugated Chalcone Derivatives: Modulation of the Effective π-Conjugated Structure, *J. Phys. Chem. A*, 2020, **124**(51), 10808–10816.

12 T. Yamamoto, Molecular assembly and properties of polythiophenes, *NPG Asia Mater.*, 2010, **2**(2), 54–60.

13 F. Kajzar and C. Y. Lee, *Photoactive organic materials*, 1996.

14 M. Rutkis, A. Jurgis, V. Kampars, A. Vembris, A. Tokmakovs and V. Kokars, New Figure of Merit for Tailoring Optimal Structure of the Second Order NLO Chromophore for Guest–Host Polymers, *Mol. Cryst. Liq. Cryst.*, 2008, **485**, 903–914.

15 A. Bundulis, E. Nitiss, I. Mihailovs, J. Busenbergs and M. Rutkis, Study of Structure-Third-Order Susceptibility Relation of Indandione Derivatives, *J. Phys. Chem. C*, 2016, **120**(48), 27515–27522.

16 V. Ramkumar, S. Anandhi, P. Kannan and R. Gopalakrishnan, Substitution effect on chalcone based materials for corrosion and photocrosslinking applications, *RSC Adv.*, 2014, **5**(1), 586–596.

17 V. Ramkumar, S. Anandhi, P. Kannan and R. Gopalakrishnan, Synthesis, single crystal growth, characterization and comparison of two new enone shifted chalcones and their NLO behaviour, *CrystEngComm*, 2013, **15**(13), 2438–2449.

18 J. P. Abraham, D. Sajan, V. Shettigar, S. M. Dharmaprakash and V. S. Jayakumar, Efficient π-electron conjugated push–pull nonlinear optical chromophore 1-(4-methoxyphenyl)-3-(3,4-dimethoxyphenyl)-2-propen-1-one: A vibrational spectral study, *J. Mol. Struct.*, 2009, **917**(1), 27–36.

19 T. Kogej, D. Beljonne, F. Meyers, J. W. Perry, S. R. Marder and J. L. Brédas, Mechanisms for enhancement of two-photon absorption in donor–acceptor conjugated chromophores, *Chem. Phys. Lett.*, 1998, **298**(1), 1–6.

20 H. E. Katz, K. D. Singer, J. E. Sohn, C. W. Dirk, L. A. King and H. M. Gordon, Greatly enhanced second-order nonlinear optical susceptibilities in donor-acceptor organic molecules, *ChemInform*, 1988, **19**(6), 6561–6563.

21 Q. Bellier, N. S. Makarov, P.-A. Bouit, S. Rigaut, K. Kamada, P. Feneyrou, G. Berginc, O. Maury, J. W. Perry and C. Andraud, Excited state absorption: a key phenomenon for the improvement of biphotonic based optical limiting at telecommunication wavelengths, *Phys. Chem. Chem. Phys.*, 2012, **14**(44), 15299–15307.

22 Z. Liu, S. Hua and X. Yan, Linear and Nonlinear Optical Properties of Triphenylamine–Indandione Chromophores: Theoretical Study of the Structure–Function Relationship under the Combined Action of Substituent and Symmetry Change, *J. Phys. Chem. A*, 2018, **122**(9), 2344–2352.

© 2022 The Author(s). Published by the Royal Society of Chemistry

23 D. Gudeika, A. Bundulis, I. Mihailovs, D. Volyniuk, M. Rutkis and J. V. Grazulevicius, Donor and acceptor substituted triphenylamines exhibiting bipolar charge-transporting and NLO properties, *Dyes Pigm.*, 2017, **140**, 431–440.

24 M. Rutkis, A. Vembris, V. Zauls, R. Tokmakovs, E. Fonavs, R. Jurgis and V. Kampars, Novel second-order non-linear optical polymer materials containing indandione derivativatives as a chromophore, *Conference on Organic Optoelectronics and Photonics II*, 20060403-06, Strasbourg (FR), Institute of Solid State Physics, University of Latvia, 8 Kengaraga St. LV, 2006, vol. 1063, pp. 61922Q.1–61922Q.8.

25 A. V. Kulinich, N. A. Derevyanko, E. K. Mikitenko and A. A. Ishchenko, Merocyanines based on 1,3-indandione: electronic structure and solvatochromism, *J. Phys. Org. Chem.*, 2011, **24**(8), 732–742.

26 I. Mihailovs, J. Kreicberga, V. Kampars, S. Miasojedovas, S. Juršenas, L. Skuja and M. Rutkis, Hyper-Rayleigh scattering and two-photon luminescence of phenylamine–indandione chromophores, *IOP Conf. Ser.: Mater. Sci. Eng.*, 2012, **38**, 012035.

27 V. Zilinskaite, D. Gudeika, J. V. Grazulevicius, D. Volyniuk, G. Buika, V. Jankauskas, G. Juska, M. Rutkis and A. Tokmakov, Derivatives of indandione and differently substituted triphenylamine with charge-transporting and NLO properties, *Dyes Pigm.*, 2015, **113**, 38–46.

28 M. Olivucci, *COMPUTATIONAL PHOTOCHEMISTRY*, Elsevier, 2005.

29 A. V. Arbuznikov, Hybrid exchange correlation functionals and potentials: Concept elaboration, *J. Struct. Chem.*, 2007, **48**(1 Supplement), S1–S31.

30 S. Tian, Y.-Z. Li, M.-B. Li, J. Yuan, J. Yang, Z. Wu and R. Jin, Structural isomerism in gold nanoparticles revealed by X-ray crystallography, *Nat. Commun.*, 2015, **6**(1), 8667.

31 R. Berera, R. van Grondelle and J. T. M. Kennis, Ultrafast transient absorption spectroscopy: principles and application to photosynthetic systems, *Photosynth. Res.*, 2009, **101**(2), 105–118.

32 K. Wang, A. Vezzoli, I. M. Grace, M. McLaughlin, R. J. Nichols, B. Xu, C. J. Lambert and S. J. Higgins, Charge transfer complexation boosts molecular conductance through Fermi level pinning, *Chem. Sci.*, 2019, **10**(8), 2396–2403.

33 X. Wu, J. Xiao, S. Ru, T. Jin and Y. Song, Spindle-Type Conjugated Compounds Containing Twistacene Unit: Synthesis and Ultrafast Broadband Reverse Saturable Absorption, *Adv. Opt. Mater.*, 2017, **5**(2), 1600712.

34 I. H. M. van Stokkum, D. S. Larsen and R. van Grondelle, Global and target analysis of time-resolved spectra, *Biochim. Biophys. Acta, Bioenerg.*, 2004, **1657**(2), 82–104.

35 L. Shen, Z. Li, X. Wu, W. Zhou, J. Yang and Y. Song, Ultrafast broadband nonlinear optical properties and excited-state dynamics of two bis-chalcone derivatives, *RSC Adv.*, 2020, **10**(26), 15199–15205.

36 S.-t. Shi, Y. Fang, J.-y. Yang, Y.-b. Han and Y.-l. Song, The remarkable enhancement of two-photon absorption in pyrene based chalcone derivatives, *Opt. Mater.*, 2018, **86**, 331–337.

37 W. Zhou, Y. Fang, X. Wu, Y. Han, J. Yang, L. Shen and Y. Song, Anthracene derivatives as broadband nonlinear optical materials: nonlinear absorption and excited-state dynamics analysis, *RSC Adv.*, 2020, **10**(34), 19974–19981.

38 P. Poornesh, G. Umesh, P. K. Hegde, M. G. Manjunatha, K. B. Manjunatha and A. V. Adhikari, Studies on third-order nonlinear optical properties and reverse saturable absorption in polythiophene/poly(methylmethacrylate) composites, *Appl. Phys. B*, 2009, **97**(1), 117–124.

39 C. Peter, L. Yi and Å. Hans, Generalized few-state models for two-photon absorption of conjugated molecules, *Chem. Phys. Lett.*, 2002, **352**(3–4), 262–269.

40 Z. Xiao, Y. Shi, R. Sun, J. Ge, Z. Li, Y. Fang, X. Wu, J. Yang, M. Zhao and Y. Song, Ultrafast broadband optical limiting in simple pyrene-based molecules with high transmittance from visible to infrared regions, *J. Mater. Chem. C*, 2016, **4**(21), 4647–4653.

41 M. Sheik-Bahae and A. A. Said, Sensitive measurement of optical nonlinearities using a single beam, IEEE, *IEEE J. Quantum Electron.*, 1990, **26**(4), 760–769.

42 R. Niu, S. Chen, W. Zhou, X. Wu, J. Yang, Y. Wang, X. Zhang and Y. Song, Modulation of trithiophene-based chalcone positional isomers by twist angle variation: Ultrafast nonlinear optical properties and excited-state dynamics, *J. Photochem. Photobiol., A*, 2021, **411**(113210), 33–38.

43 P. Feneyrou, O. Doclot, D. Block, P. L. Baldeck and S. Delysse, Characterization of the two-photon absorption resonance that is due to the internal charge-transfer transition of a push–pull molecule, 4-(diethylamino)-β-nitrostyrene, *Opt. Lett.*, 1997, **22**(15), 1132–1134.

44 J. Y. Yang, Y. L. Song, Y. X. Wang, C. W. Li, X. Jin and M. Shui, Time-resolved pump–probe technology with phase object for measurements of optical nonlinearities, *Opt. Express*, 2009, **17**(9), 7110–7116.

45 W. J. Tan, H. Liu, J. H. Si and X. Hou, Control of the gated spectra with narrow bandwidth from a supercontinuum using ultrafast optical Kerr gate of bismuth glass, *Appl. Phys. Lett.*, 2008, **93**(5), 051109.

46 X. Wu, J. Yang, Z. Xiao, Y. Yang, F. Zhou and Y. Song, Effect of Fe-doping on nonlinear optical responses and carrier trapping dynamics in GaN single crystals, *Appl. Phys. Lett.*, 2015, **107**(5), 051901.

47 Y. Fang, Z. Xiao, X. Wu, F. Zhou, J. Yang, Y. Yang and Y. Song, Optical nonlinearities and ultrafast all-optical switching of m-plane GaN in the near-infrared, *Appl. Phys. Lett.*, 2015, **106**(25), 251903.

48 M. Pawlicki, H. A. Collins, R. G. Denning and H. L. Anderson, Two-Photon Absorption and the Design of Two-Photon Dyes, *Angew. Chem., Int. Ed.*, 2009, **48**(18), 3244–3266.